

# THE USE OF AN RF UNDULATOR IN THE DESIGN OF AN ACCELERATING STRUCTURE

N. V. Avreline, TRIUMF, Vancouver, Canada

S. M. Polozov, A. G. Ponomarenko, National Research Nuclear University MEPhI (Moscow Engineering Physics Institute), Moscow, Russia

## Abstract

The idea of accelerating a beam in the accelerating structures based on an RF undulator poses great advantages in high current proton and ions accelerators. The accelerating structure based on an RF undulator uses a combinational wave that consists of the zeroth and the first harmonics for acceleration and focusing. This paper presents the development of this accelerating structure for acceleration of a beam. In particular, we show that this structure is an H-type resonator composed from five coupled sections.

## INTRODUCTION

This paper describes the design of new accelerating structures for acceleration of high current ion beams that use a combinational wave consisting of RF field's zeroth and the first spatial harmonics. This type of accelerator belongs to the class of longitudinal RF undulator accelerators [1] and is the next step in the logical development of the idea of undulator-based accelerating structures proposed earlier. The analytical studies of them have already been published in [2-4]. The undulator acceleration mechanism is similar to the acceleration mechanism in an inverse free electron laser (IFEL) [5], where ponderomotive forces accelerate an electron beam.

## ACCELERATION IN RF UNDULATOR

The proposed structure utilizes the RF undulator with the zeroth and the first spatial harmonics providing the acceleration and focusing of a proton beam. One of the advantages of this structure is that it allows to simultaneously accelerate two ion beams with ions of different polarity (protons and negative ions of hydrogen). In the later stages of acceleration, bunches of particles of opposite polarity accelerate separately in different synchronous phases [3]. In this paper, we will discuss the acceleration of just the proton beam, as the results for the negative hydrogen ion beam are similar and differ only in the phase. The electrical components of the fringe fields near edges of the drift tubes play the role of focusing and defocusing lenses for the beam. As these lenses are separated by the distance of the accelerating gap, they result in a net focusing effect. The other focusing factor is travel time in these lenses. The protons travel through focusing lenses slower than through defocusing lenses, as a result of the energy gain in the gap. So once again, the overall net effect is beam focusing. The proposed structure could accelerate proton beam from injection energy of 46 keV to energy of 543 keV. The length of this structure is 1258 mm. The dimensions of the accelerating gaps and the length of drift tubes determine the ratio of the zeroth ( $E_0$ ) and the first harmonics

( $E_1$ ):  $\chi = E_1/E_0$ . The combination of these two spatial harmonics represents the combined wave that accelerates beam. The optimal value of  $\chi$  is between 0.25 and 0.3 [2], specifically we selected  $\chi = 0.25$ . We determine the ratio of structure period to accelerating gaps with the help of formula (1):

$$\chi = -\frac{\sin(\frac{3\pi h}{2D})I_0(\frac{\pi}{D}R_{t,in})}{9\sin(\frac{\pi h}{2D})I_0(\frac{3\pi}{D}R_{t,in})}, \quad (1)$$

where  $h$  – accelerating gap length,  $D$  – period length of the accelerating channel and  $R_{t,in}$  is defined in Fig. 1.

The accelerating channel has an 8 mm diameter and consists of drift tubes with outer diameter of 10 mm. Figure 1 shows the cross-section of the accelerating channel for one structure period.

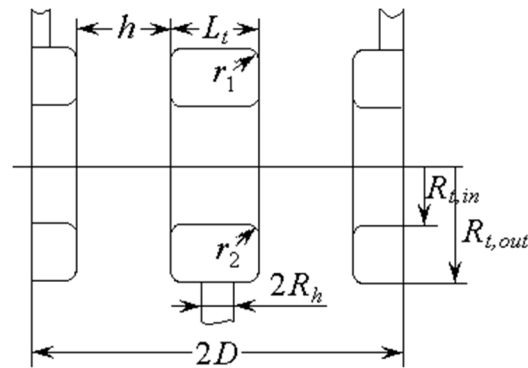


Figure 1: The period of the accelerating channel.

A specific property of the accelerating structure with undulator is that neither the zeroth harmonic, nor the first harmonic are synchronous to the synchronous particle of the beam, only the combined wave is synchronous with beam.

## Combinational Wave

Figure 2 shows the sum of the zeroth and the first spatial harmonics in coordinate system that is aligned with the position of synchronous proton for different moments of time.

This is a preprint — the final version is published with IOP

Content from this work may be used under the terms of the CC BY 3.0 licence (© 2019). Any distribution of this work must maintain attribution to the author(s), title of the work, publisher, and DOI

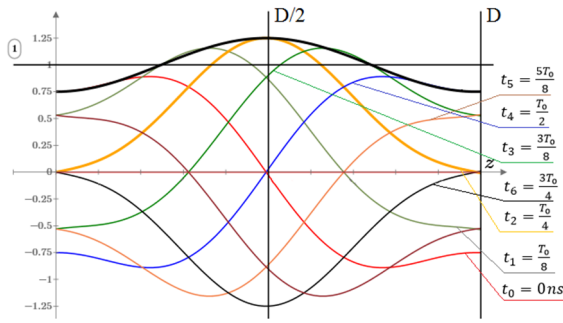


Figure 2: The composition of combined wave in one of the accelerating gaps.

Figure 2 also illustrates amplitude modulation in the sum of spatial harmonics and the maximal amplitude in one of the acceleration gaps is shown in bold. Combined wave represents the beating of the zeroth and the first spatial harmonics. Expression (2) shows the formula for the combined wave:

$$E_{com} = E_0 E_1 \cos\left(2\pi f_0 t - \frac{2\pi z}{D}\right), \quad (2)$$

Where  $E_0$  – amplitude of the zeroth spatial harmonic,  $E_1$  – amplitude of the first spatial harmonic,  $f_0$  – operational frequency of the accelerating structure,  $t$  – time.

The phase velocity of the combined wave  $\beta_s$  is one half of the zeroth spatial harmonic and is three halves of the first spatial harmonic, if the structure is in  $\pi$  mode:

$$\beta_{0,s} = 2\beta_s, \quad \beta_{1,s} = \frac{2\beta_s}{3} \quad (3)$$

The goal was to design an accelerating structure that bunches the beam at its beginning and then accelerates it in the rest of the structure. Specifically, the accelerating field grows at the beginning of the structure for better bunching and is then constant for the next part of the structure.

The results of beam dynamics calculations show that phase velocity of the combined wave grows in the direction of acceleration as is shown at Fig. 3.

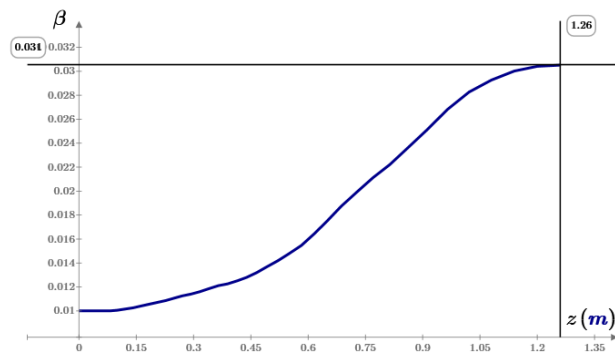


Figure 3: Phase velocity of the combined wave.

The length of period  $D$  for  $\pi$  mode is:

$$D = \beta_s(z)\lambda \quad (4)$$

The structure has 38 drift tubes; the period value varies from 20 mm to 61 mm.

Figure 4 shows how period  $D$  depends on the  $z$  coordinate.

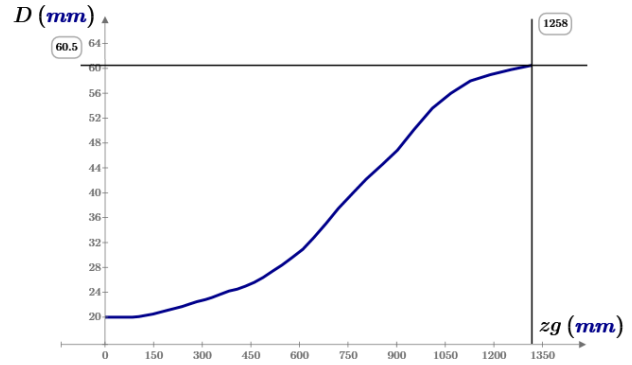


Figure 4: Period  $D$ 's dependence on coordinate  $z$ .

The synchronous phase was 67 degrees. The result of beam dynamics calculation in Astra (A Space Charge Tracking Algorithm) [6] confirms the possibility of accelerating protons that are synchronous with the combined wave. Figure 5 shows the velocity of a reference proton with respect to the  $z$  coordinate.

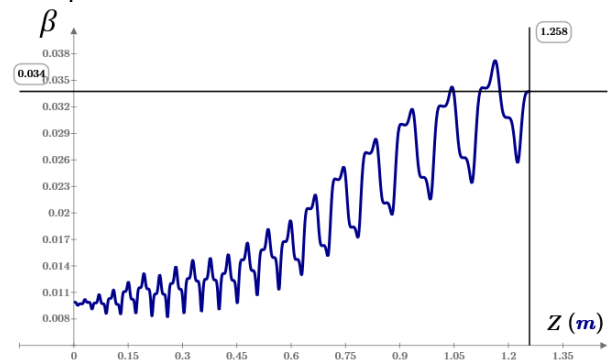


Figure 5: Velocity of synchronous proton accelerated by combined wave.

Figure 5 illustrates that the zeroth harmonic shows periodic variation in proton's velocity and also shows overall acceleration due to the combined wave.

Figure 6 shows the variation of the phase for the proton that was injected in phase equal to  $\pi/4$  (blue line) and the synchronous phase of the combined wave (red line) along the accelerating structure.

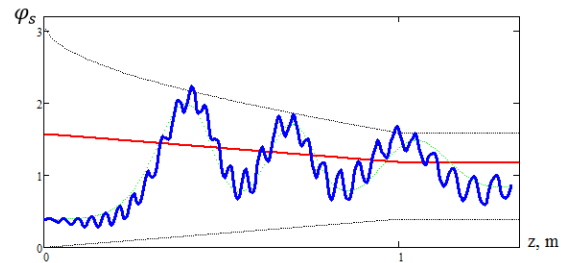


Figure 6: Variation of for proton that was inject with phase equal to  $\pi/4$  along the accelerating structure.

Content from this work may be used under the terms of the CC BY 3.0 licence (© 2019). Any distribution of this work must maintain attribution to the author(s), title of the work, publisher, and DOI

This is a preprint — the final version is published with IOP

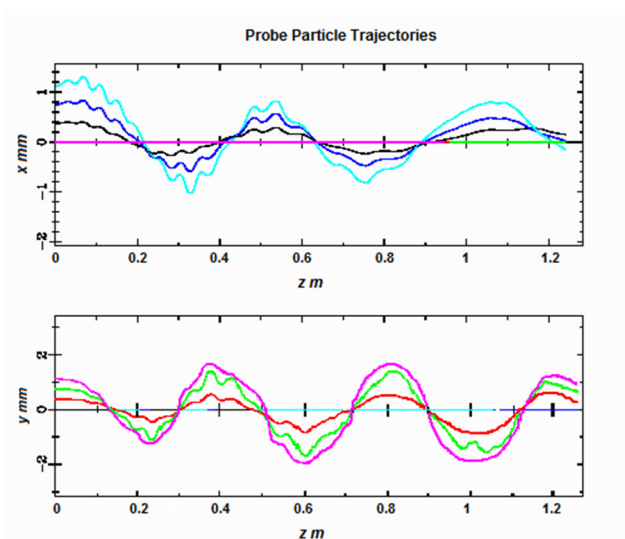


Figure 7: Probe particle trajectories.

The calculation of trajectories in Astra showed that deflections of probe protons from the central axis of the structure are less than 1.4 mm in the x direction and are less than 2 mm in the y direction (Fig. 7).

Calculations determined the current transmission coefficient to be equal to 83 %.

### Accelerating Structure

We selected H-type structure excited in  $TE_{115}$  as it has high shunt impedance and it allows tuning the required field distribution. The accelerating channel has an essential difference in the capacitance between drift tubes at the entrance of the structure and at its exit. This results in problems with tuning of the required field distribution. The structure composed of five subsections allows for greater flexibility in tuning of acceleration, especially in the cases where the field distribution increases with respect to distance. Figure 8 shows the design of the structure (subsection 1 (pos. 1), subsection 2 (pos. 2), subsection 3 (pos. 3), subsection 4 (pos. 4) and subsection 5 (pos. 5)).

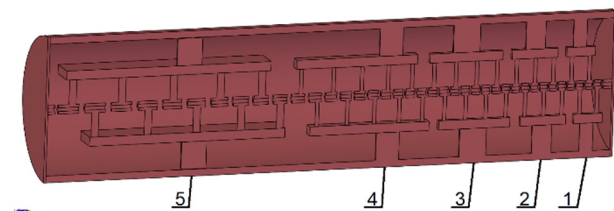


Figure 8: The accelerating structure based on RF undulator.

The inner diameter of the cavity is 296 mm, its length is 1258 mm. The accelerating structure design allows for many adjustments of the field distribution, such as changing diameters of supports (pos. 1, pos. 2, pos. 3, pos. 4 and pos. 5) and their positions along the accelerating channel.

### Tuning of RF Fields

The distribution of the RF potential on the cavity's surface of the structure along z axis is about sinusoidal for the H-type of accelerating structures which allowed to have lower accelerating field at the first accelerating gap. Then, the combination of coupling between sections, the position of supports and the shape of supports and bars allowed to reach the required field distribution. Specifically, in this distribution, the accelerating field grows in the first four sections to get gradual bunching of beam. The maximal amplitude of the RF field is  $172 \frac{kV}{cm}$ . The rate of energy gain is 420 keV/m in this accelerating structure and is higher than in the RFQ structure where the rate of energy gain is usually not greater than 300 – 400 keV/m.

Figure 9 shows the result of ANSYS HFSS simulation for distribution of electromagnetic field in this accelerating structure.

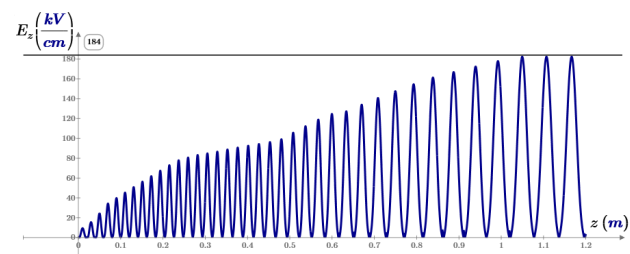


Figure 9: The  $E_z$  distribution along the axis of the accelerating structure.

The accelerating field grows along the axis of the accelerating structure and allows for the beam to bunch. The distribution of the accelerating field also shows variation in the rate of energy gain as the amplitude grows, which allows for better bunching and focusing of the beam.

The structure has  $R_{sh} = 114 \frac{M\Omega}{m}$ ,  $Q_0 = 6263$ , it is required 120 kW RF of power for operation.

The steady-state thermal simulation of the accelerating structure in ANSYS Workbench showed that it is able to operate in pulse mode with duty factor equal to 10%, when all bars except the first section are water-cooled. Maximal temperature in this regime would be below 78 °C.

The static structural simulation in ANSYS Workbench of this structure showed that its maximal thermal deformation would be below 100  $\mu m$ .

### CONCLUSION

This paper discussed the fundamentals of design, the results of beam dynamics calculations and the results of simulation of the accelerating structure in ANSYS HFSS for UNDULAC-RF design based on H-type cavity resonator operating in  $TE_{115}$  mode. The results confirm the practicality of building this kind of accelerator. The accelerating section of this accelerating structure would allow accelerating beams from 46 kV to 543 keV. The best applications of this structure are in LINAC for simultaneous acceleration of proton and negative hydrogen ion beams.

This is a preprint — the final version is published with IOP

Content from this work may be used under the terms of the CC BY 3.0 licence (© 2019). Any distribution of this work must maintain attribution to the author(s), title of the work, publisher, and DOI

## REFERENCES

- [1] E. S. Masunov and S. M. Polozov, “Dynamics of the two-component ion beam in a linear undulator accelerator”, *Technical Physics*, vol. 54, no. 8, pp. 1179–1184, 2009.
- [2] E. S. Masunov, N. V. Avreline, V. S. Dyubkov, S. M. Polozov, and A. L. Sitnikov, “Choice of Accelerating System for Undulator Linear Accelerator”, in *Proc. 11th European Particle Accelerator Conf. (EPAC'08)*, Genoa, Italy, Jun. 2008, paper THPP040, pp. 3455-3457.
- [3] E. S. Masunov, *Technical Physics*, vol. 79, no. 8, pp. 93 – 98, 2009.
- [4] E. S. Masunov, *Technical Physics*, vol. 46, no. 11, pp. 1433 – 1436, 2001.
- [5] T. C. Marshall *et al.*, “Inverse FEL accelerator: experiment and theory”, *Nucl. Int. Meth. Phys.*, vol. 304, no. 1–3, pp. 683-686, 1991.
- [6] ASTRA “A Space Charge Tracking Algorithm”, 2017, [http://www.desy.de/~mpyflo/Astra\\_manual/Astra-Manual\\_V3.2.pdf](http://www.desy.de/~mpyflo/Astra_manual/Astra-Manual_V3.2.pdf)

Content from this work may be used under the terms of the CC BY 3.0 licence (© 2019). Any distribution of this work must maintain attribution to the author(s), title of the work, publisher, and DOI